Superheating of Confined Pb Thin Films

L. Zhang,[1] Z. H. Jin,[1] L. H. Zhang,[2] M. L. Sui,[2] and K. Lu[1,*]

[1]*State Key Laboratory of Rapidly Solidified Non-equilibrium Alloys, Institute of Metal Research, Chinese Academy of Sciences, Shenyang 110015, China*

[2]*Laboratory of Atomic Imaging of Solids, Institute of Metal Research, Chinese Academy of Sciences, Shenyang 110015, China*

(Received 1 March 2000)

In this work we report, for the first time, an experimental observation of a superheating phenomenon in metal thin films. By means of cold rolling, Pb thin films of about 20 nm thick were sandwiched by Al layers, and between them semicoherent epitaxial Pb/Al interfaces were formed. *In situ* x-ray diffraction analysis indicated that the confined Pb thin films could be superheated for at least 6 °C. Thermodynamic analysis indicated that such a substantial superheating in the confined two-dimensional thin films may originate from suppression of growth of the molten droplets by the epitaxial Al/Pb/Al confinement, instead of suppression of melt nucleation for the confined particle superheating.

PACS numbers: 68.55.–a, 61.10.–i, 68.35.Rh, 64.70.Dv

It is well known that melting points of low-dimensional solids, such as nanoparticles, thin films, nanofibers, etc., are considerably reduced relative to the equilibrium melting point (T_m) of bulk solids. For example, the melting point of free-standing nanoparticles and thin films may be as little as half of the bulk material [1–3]. It has been repeatedly emphasized that melting of a solid is initiated by melt nucleation at the solid surfaces or interfaces that occurs normally below its equilibrium T_m [4–6]. When the dimension of a solid is reduced, or in other words, more surfaces and interfaces are provided where heterogeneous nucleation of melt may take place, the melting temperature will be lowered. Meanwhile more and more low-dimensional materials have found applications in modern industries, their stability against melting is becoming one of the major concerns in further development and applications of this new materials family. Exploration of possible approaches to elevate the instability (melting) temperature of the low-dimensional materials will be of great significance for both the technological applications and the fundamental understanding of the melting mechanism.

Elevating melting points of metal particles has been successfully realized in a number of metal systems [7–13] when the particles are coated by (or embedded in) a high-T_m metal with epitaxial particle/matrix interfaces. Suppression of heterogeneous nucleation of melt at the epitaxial interfaces with a low interfacial energy is supposed to be a key factor to control the superheating [4,13–15].

However, for two-dimensional (2D) thin films, those necessary conditions for superheating of particles could not be practically feasible. Even if a thin film could be sandwiched by two high-T_m films with coherent or semicoherent interfaces, heterogeneous nucleation of melt at various defects in the film (film bounds, grain boundaries) and at the defective interfaces would not be effectively suppressed. Therefore, 2D thin films are usually regarded to be hardly superheated.

In this work we report, for the first time, an observation of a substantial superheating in confined Pb thin films sandwiched by Al. Such a superheating phenomenon in the thin film is attributed to suppression of a melt growth by the epitaxial Al/Pb/Al confinement, instead of suppression of melt nucleation in the case of confined particles. This effect may provide new possibilities to elevate the instability temperature against melting for other low-dimensional materials (e.g., films and wires) of increasingly technological interests.

Elemental pure Al and Pb foils of about 20 μm thick and 10 mm wide, with the same purity of 99.99%, were alternatively stacked to make an Al/Pb/Al sandwich. The Al/Pb/Al sandwich was repeatedly rolled and folded at ambient temperature until the nominal thickness of Pb layers was reduced into the nanometer regime. At intervals the sample was annealed at 320 °C to eliminate work hardening of Al. Finally, the as-rolled Pb/Al samples were annealed at 320 °C for 30 min in order to release the strain and stabilize the Pb/Al interface structure.

Structure characterization by means of x-ray diffraction (XRD) analysis (on a Rigaku D/Max 2400 x-ray diffractometer operated at 150 mA, 50 kV with Cu K_α radiation) indicated that only pure Pb and Al are detectable in the as-rolled Pb/Al sample. The lattice parameter measurements indicated that no solid solution was formed between these two immiscible elements upon cold rolling. Transmission electron microscopy (TEM) (on a JEM-2010 transmission electron microscope with an accelerating voltage of 200 kV) observations showed that in the rolled Pb/Al specimens, Pb was deformed into thin films sandwiched by Al layers. But the Pb films are fragmentary rather than continuous layers throughout the rolled strip. Plan-view TEM images showed that the size of each Pb (polycrystalline) fragment ranges from about a few hundred nanometers to a few microns, in which the Pb grain size is about ~50–70 nm. Cross-sectional TEM images indicated that the thickness of most Pb fragment layers is rather uniform, being about 20 ± 5 nm [as shown in Fig. 1(a)].

 0031-9007/00/85(7)/1484(4)$15.00

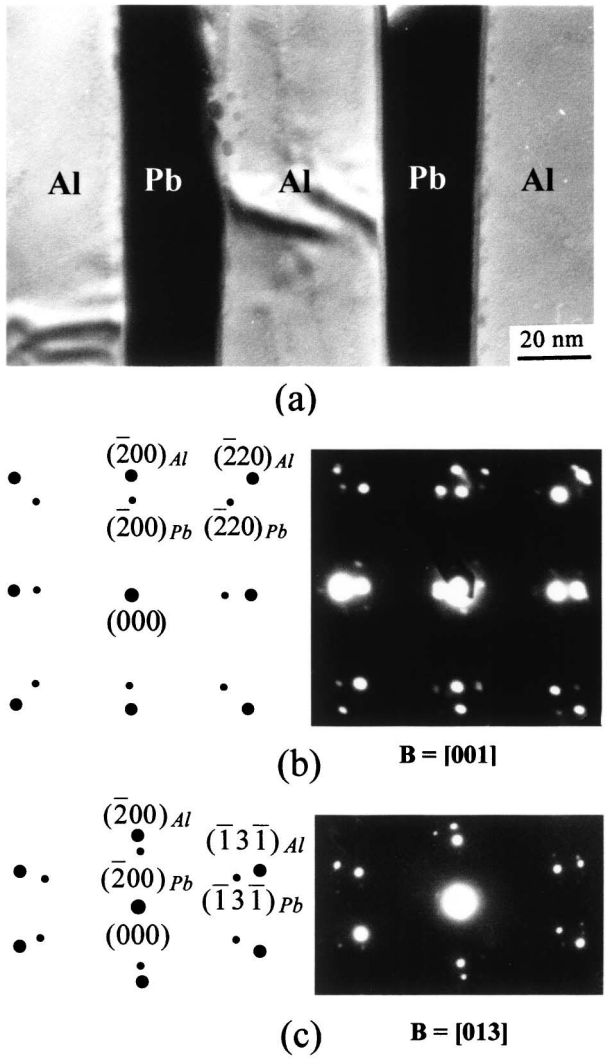

FIG. 1. A cross-sectional TEM observation of the Pb/Al multilayer thin film sample (a); SAED patterns and their indexed patterns for the Pb/Al sample along Pb ⟨001⟩ (b) and ⟨013⟩ (c) directions. The unindexed spots in the SAED patterns are the double diffraction spots.

From selected area electron diffraction (SAED) patterns of the Pb/Al thin films, we found that for most Pb fragment layers no specific crystallographic orientation relationship exists between the Pb and Al phases. But for a small fraction of Pb layers, a cubic-cubic orientation relationship between Pb and Al was detected, as shown in Figs. 1(b) and 1(c). That provides an evidence for existence of the semicoherent Pb/Al interfaces. Such an epitaxial Pb/Al interface is consistent with that observed in the Pb particles embedded in the Al matrix synthesized by means of melt quenching [9,13] and ion implantation [12].

In situ XRD was employed to monitor the melting process of the confined Pb films during heating on the same diffractometer equipped with a high-temperature attachment. For comparison, a thin pure lead foil with a thickness of about 10 μm was also prepared by means of rolling. Specimens with a size of 4 × 5 mm were fixed on an Al sample holder, which was then mounted on a platinum bearing frame and kept under vacuum condition (10^{-3} Pa). A thermocouple (Pt and Pt-Rh 13%) was embedded in the platinum frame, contacting with the Al sample holder. The sample temperature was controlled with an accuracy of ±1 °C. It took about 2 min to measure a 4° span for every selected Pb Bragg diffraction, i.e., (111), (200), (220), and (331) at an angular step of $2\theta = 0.02°$.

Figures 2(a) and 2(b) show the XRD diffraction profiles of the Pb/Al sample and the pure Pb foil at different temperatures around the equilibrium T_m of Pb (327.3 °C), respectively. It is seen that the intensity of (111) and (200) peaks vanishes abruptly between 327 °C and 329 °C for pure Pb, indicating the solid Pb completely melted. It also reflects the accuracy of the temperature control (±1 °C) in the present measurement. For the Al/Pb/Al multilayer sample, the intensity of (111), (200), and (220) decreases at elevating temperatures, but these peaks can still be identified at 329 °C. The integrated intensity of (111) reflection was reduced by about 80% at 329 °C relative to

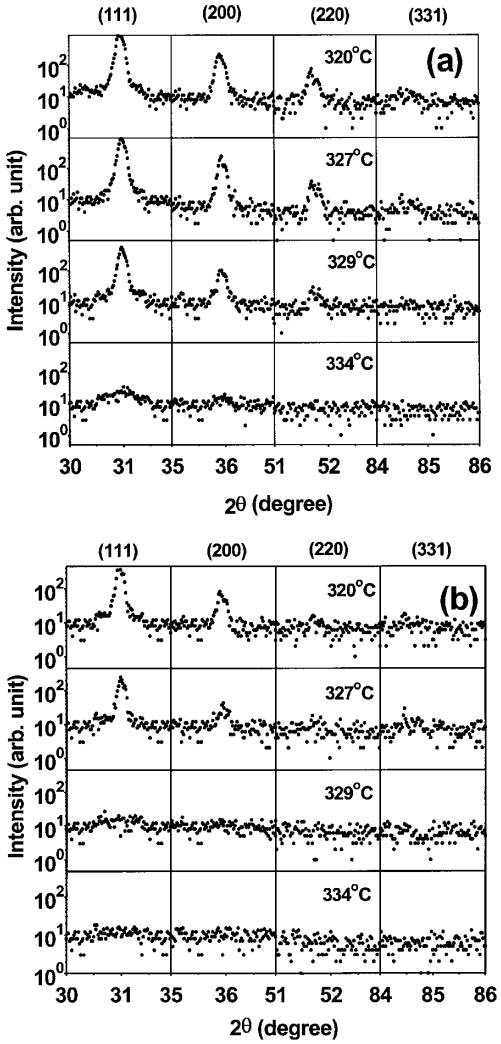

FIG. 2. XRD profiles of Pb (111), (200), (220), and (331) at different temperatures (as indicated) for the Pb/Al sample (a) and for the pure Pb film sample (b).

that at 327 °C, implying a considerable fraction of solid Pb in the sample has melted at ~327–329 °C, while a small fraction of solid Pb exhibits an enhanced stability against melting. At 334 °C, the (111) diffraction is still visible while other peaks have completely disappeared.

Figure 3 displays the variation of the integrated intensity of four profiles with temperature for the Pb/Al sample as well as the pure Pb samples. Evidently, all Bragg diffraction lines in the pure Pb sample disappeared below 329 °C. In the Pb/Al sample, evident diffraction profiles can be observed above the equilibrium T_m. Such a reduction of diffraction intensity is mainly attributed to a decrease of the volume fraction of the remaining Pb crystals, as the reduction induced by the Debye factor is relatively small in this temperature range. The temperatures at which the XRD profiles disappear at 6, 2, and 1 °C above equilibrium T_m for (111), (200), and (220) reflections, respectively. It means that some solid Pb films can be superheated for at least 6 °C relative to bulk $T_m = 328$ °C. The same experiment has been repeated for several times using different Pb/Al specimens, and rather consistent results were obtained. The largest superheating observed in the Pb/Al samples varies in a range of ~3–10 °C [in (111) reflection]. Since it took about 50 min to carry out the *in situ* XRD measurements from 328 to 334 °C, such a superheating of a few degrees is a substantial metastable superheating, rather than an unstable kinetic superheating due to the time limit [16].

According to the structure characterization of the rolled Pb/Al specimen, one can deduce that the melting of solid Pb below 329 °C is from those Pb films without an orientation relationship at Pb/Al interfaces where melt nucleation and growth are easily occurring, while the superheated solid Pb might be the film with semicoherent Pb/Al interfaces as identified by SAED analysis. Previous studies [9,10,13] indicated that the superheating of Pb nanoparticles embedded in the Al matrix usually originates from two effects: (1) epitaxial semicoherent Pb/Al interfaces that suppress the nucleation of melt at particle surfaces, and (2) an increasing pressure on Pb particles (due to different thermal expansion coefficients between solid Pb and Al) at elevating T_m.

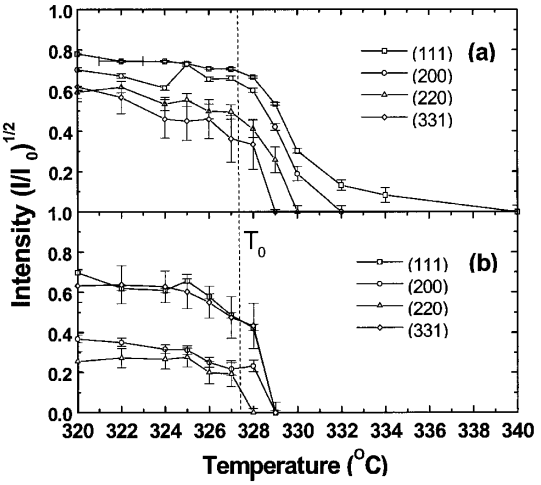

FIG. 3. Variation of the XRD profiles intensity with temperature for the Pb/Al sample (a) and the pure Pb foil (b). The dashed line indicates the equilibrium bulk T_m of Pb.

In order to evaluate the effect of pressure on the superheating, lattice parameter measurements were carried out in the Pb/Al thin film sample, as usually done in the cases of embedded nanoparticles. The measured lattice parameter of the confined Pb film at 327 °C (below the equilibrium melting point) is $a = 4.995 \pm 0.001$ Å. The tabulated value of lattice parameter for bulk Pb at this temperature is 4.9957 Å [10]. It is evident that these values are rather consistent, implying that the additional pressure imposed on the sandwiched Pb films is essentially negligible.

Then, it is reasonable to attribute the observed superheating of Pb in our *in situ* XRD experiments to the Pb films with epitaxial semicoherent Pb/Al interfaces. As proven by experimental studies and computer simulations, nucleation of Pb melt at the epitaxial Pb/Al interface could be suppressed [13,17]. Suppression of melt nucleation plays a dominant role in achieving superheated nanoparticles. However, in the case of thin films, nucleation of melt may not be prevented due to various kinds of defects existing in the polycrystalline films and at the Pb/Al interfaces.

The melting of a solid is a kinetic process consisting of nucleation and growth of the molten phase. Even though the melt nucleation in the thin films could not be prevented, growth of the molten phase might be suppressed by the special confinement. From a thermodynamic point of view, the driven force (ΔG) for growth of a melt droplet nucleated at the defective interfaces comes from the Gibbs free energy change due to the solid to liquid transition. But owing to the confinement of the thin film by semicoherent Pb/Al interfaces which possess a low Pb/Al interfacial energy, the melt front interface should be curved (as schematically shown in Fig. 4) as $\gamma_{\mathrm{Pb}(s)\mathrm{Al}} + \gamma_{\mathrm{Pb}(s)\mathrm{Pb}(l)} \cos(\theta) = \gamma_{\mathrm{Pb}(l)\mathrm{Al}}$. The wetting angle ($\theta$) is less than 90° as $\gamma_{\mathrm{Pb}(s)\mathrm{Al}} < \gamma_{\mathrm{Pb}(l)\mathrm{Al}}$ due to the Pb/Al epitaxy.

In order to overcome the interfacial energy difference $\Delta\gamma = \gamma_{\mathrm{Pb}(l)\mathrm{Al}} - \gamma_{\mathrm{Pb}(s)\mathrm{Al}}$ during the growth of a melt, an excess work $\Delta W = 2\Delta\gamma$ must be done to maintain the critical driving force per unit Pb/Al interface area, which will result in an elevation of the melting point (ΔT). Based on the thermodynamic analysis, the superheating temperature (ΔT) for a melt growth within a thin film can be obtained via the equation:

$$\Delta T = \frac{2\gamma_{sl} T_m \cos^2\theta}{D L_V (\pi/2 - \theta)},$$

where D is the film thickness, L_V is the latent heat per unit volume, θ is the wetting angle (see Fig. 4), and γ_{sl} is the solid/liquid interfacial energy.

For the Pb layers of 20 nm thick, the melting point elevation due to this excess work was estimated to be about

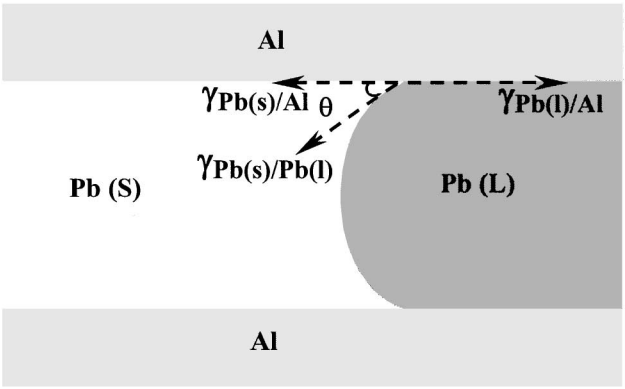

FIG. 4. A schematic illustration of interfacial conditions for the growth of a Pb liquid droplet, formed at defective interfaces in the Pb film confined by Al layers.

$\sim$9–2 °C when $\theta = 0 \sim 80°$ and $\gamma_{sl} = 0.05$ J/m^2. Such an evaluation coincidences reasonably with the observed superheating in our Pb/Al samples.

In addition, melting of a solid is accompanied by an elastic strain energy change, which gives another resistance to the melting process [14–18]. This effect is significant for superheating of embedded nanoparticles. When the strain energy effect is taken into account in the case of thin films, an extra metastable superheating may result. For the present Pb/Al samples, this effect might be minor due to the existence of various kinds of defects in the Pb films and the Pb/Al interfaces, which can release the strain energy rather easily.

From the above analysis it is clear that the resistance to the growth of melt depends strictly upon the degree of the confinement of the Pb thin films, namely, the epitaxy at the Pb/Al interfaces. When the epitaxy at the Pb/Al interfaces is broken, the resistance to both the nucleation and the growth of melt would be out of function. Therefore, a well confinement is necessary for obtaining superheating in 2D thin film. Based on this analysis, it is anticipated that with a reduction of the film thickness, or a decrease of the epitaxial interface energy, the extent of superheating would be increased as the resistance to melt growth is enhanced.

In summary, we observed an evident superheating in a 2D Pb thin film confined by Al layers, with which epitaxial semicoherent Pb/Al interfaces are formed. The superheating of Pb thin films could be understood in terms of suppression of the growth of the molten phase by the epitaxial confinement, which provides new possibilities to elevate the instability temperature of low-dimensional materials against melting.

We gratefully acknowledge the financial support from the National Science Foundation of China (Grants No. 59801011, No. 59931030, and No. 59841004), the Ministry of Science and Technology of China (Grant No. 1999064505), and the Max-Planck Society of Germany.

*To whom correspondence should be addressed.
Email address: kelu@imr.ac.cn

[1] P. R. Couchman and W. A. Jesser, Nature (London) **269**, 481 (1977).
[2] M. Takagi, J. Phys. Soc. Jpn. **9**, 359 (1954).
[3] Ph. Buffat and J.-P. Borel, Phys. Rev. A **13**, 2287 (1976); Q. Jiang, H. Y. Tong, D. T. Hsu, K. Okuyama, and F. G. Shi, Thin Solid Films **312**, 357 (1998).
[4] R. W. Cahn, Nature (London) **323**, 668 (1986).
[5] R. W. Cahn, Nature (London) **342**, 619 (1989).
[6] B. Pluis, A. W. Denier Van Der Gon, and J. F. Van Der Veen, Surf. Sci. **239**, 265 (1990).
[7] J. Däges, H. Gleiter, and J. H. Perepezko, Phys. Lett. A **119**, 79 (1986).
[8] H. Saka, Y. Nishikawa, and T. Imura, Philos. Mag. A **57**, 895 (1988).
[9] D. L. Zhang and B. Cantor, Philos. Mag. A **62**, 557 (1990); Acta Metall. Mater. **39**, 1595 (1991).
[10] L. Gråbaek and J. Bohr, Phys. Rev. Lett. **64**, 934 (1990).
[11] R. Goswami and K. Chattopadhyay, Philos. Mag. Lett. **68**, 215 (1993).
[12] H. H. Anderson and E. Johnson, Nucl. Instrum. Methods Phys. Res., Sect. B **106**, 480 (1995).
[13] H. W. Sheng, G. Ren, L. M. Peng, Z. Q. Hu, and K. Lu, Philos. Mag. Lett. **73**, 164 (1996).
[14] K. Lu and Y. Li, Phys. Rev. Lett. **80**, 4474 (1998).
[15] U. Dahmen, S. Q. Xiao, S. Paciornik, E. Johnson, and A. Johansen, Phys. Rev. Lett. **78**, 471 (1997).
[16] J. W. Herman and H. E. Elsayed-Ali, Phys. Rev. Lett. **69**, 1228 (1992).
[17] Z. H. Jin, H. W. Sheng, and K. Lu, Phys. Rev. B **60**, 141 (1999).
[18] G. L. Allen, W. W. Gile, and W. A. Jesser, Acta Metall. **28**, 1695 (1980); D. R. Uhlmann, J. Non-Cryst. Solids **41**, 347 (1990).